IOP Conf. Series: Materials Science and Engineering **181** (2017) 012025 doi:10.1088/1757-899X/181/1/012025

Analysis of the complex stress state during early loading in cylindrical compression-shear specimens

S Pfeiffer, P Frint and M F-X Wagner

Institute of Materials Science and Engineering, Chemnitz University of Technology, 09125 Chemnitz, Germany

Abstract. In most engineering applications, materials are subjected to complex load cases rather than the simple uniaxial ones typically used for material characterization. To experimentally study the material behavior under a combination of compression and shear, an inclined compression specimen can be used. This specimen has been applied in various earlier experimental studies, typically to investigate shear localization under quasi-static or impact loading. In this contribution, we analyze the stress state in a compression-shear specimen in detail using an elastic-ideal plastic finite element simulation. The effects of specimen aspect ratio (height/diameter), inclination angle, and friction conditions between specimen and tool plates are investigated using the material parameters of different conventional steels as input. Shear stress distributions in characteristic shear directions on specific planes in the specimen that control the subsequent plastic deformation behavior are evaluated. Our results show that, even in the absence of friction, shear stresses are distributed heterogeneously in the inclined specimen, which differs from the stress distribution in a conventional compression specimen. Moreover, the highest shear and equivalent stresses always occur at the edges of the short diagonal plane of the specimen, independent of the investigated parameters. This study contributes to a more detailed understanding of the elasto-plastic mechanics in compression-shear specimens, and it specifically provides information for the analysis of the onset of early plastic deformation.

1. Introduction

Structural components face complex stress states in most applications. Industrial forming processes, impact loading and ductile fracture are just a few examples. One load case of special interest is the combination of compressive and shear loading. Different tests have been developed to investigate material behavior under such specific loading conditions. Rittel et al. [1] developed the shear-compression specimen (SCS) for large strains and a wide range of strain rates. The SCS was for instance used by Sang et al. [2] investigating a 7050 aluminum alloy, and by Moemi et al. [3] to study an AZ31 magnesium alloy, both at high temperatures. This cylindrical specimen has two notches, machined under an angle of 45° with respect to the longitudinal axis that defines the gage section. Finite element (FE) simulations show that stresses and strains are both distributed relatively uniformly within the gage section [1]. Ashab et al. [4] presented special fixtures, consisting of a support and a loading block, that can be used in universal testing machines to apply a combined compression-shear loading. Three different sets of fixtures with loading angles of 15°, 30° and 45° were used to investigate aluminum honeycomb structures, [4]. Meyer et al. [5] introduced another variation of a compression-shear specimen: The specimen (with the shape of an inclined cylinder, see figure 1) was originally developed to investigate the material behavior under combined compression and shear loading at high strain rates, with a special focus on adiabatic shear failure [6]. Recently Elibol and

Wagner [7, 8] applied this specimen geometry in static tests to study the localized phase transformation in NiTi shape memory alloys. The compression-shear specimen also allows the characterization of anisotropic material behavior under combined shear and compressive loading especially in textured materials [9]. It can be used in conventional testing machines, where uniaxial compressive loading results in a combined compression-shear stress state within the specimen, and the ratio of shear stresses to compressive stresses depends on the inclination angle of the specimen. A first analytical, but considerably simplified assessment of shear and compressive load was presented in [9], demonstrating that an inclination angle of 6° results in a shear to compressive load ratio of about 0.1. FE simulations of a similar specimen, in comparison to a conventional (i.e., non-inclined) compression specimen showed that the highest equivalent stresses occur at the edges of the shortest connecting line between the top and bottom faces of the specimen [5]. In this study, shear strains in different orientations with respect to a global coordinate system were evaluated. For an inclination of 6°, maximum shear strains of 26 % were found. Moreover, these simulations predict that the highest shear strains do not occur in a shear plane at an inclination of 45° with respect to the compressive load axis, which would be the case in simple compression.

While the results presented in [9] provide important information on the special stress state in compression-shear specimens, they are only valid for one specimen geometry (with an angle of inclination of 6°); moreover, friction between the tool plates and the faces of the specimen (which are known to play an important role in simple compression testing) have not yet been addressed. In the present study, we perform a more detailed analysis of the stress state in compression-shear specimens. We investigate different specimen inclination angles, different specimen aspect ratios (height/diameter), friction conditions and material parameters. A fully three-dimensional FE simulation, considering elastic–ideal plastic material behavior as well as contact and friction between the tool plates and the specimen, enables an in-depth analysis of the present stress state. The goal of our study is to contribute to a more detailed understanding of the mechanics of the compression-shear specimen. Based on the results of our elastic FE simulations, an assessment of the subsequent onset of early plastic deformation can be performed.

2. Specimen geometry and material parameters

The geometry of a compression-shear specimen can be fully described by the height of the specimen h, its radius r (or diameter d), and inclination angle α (see figure 1a). The geometry corresponds to a cylinder with a longitudinal axis that is inclined to the parallel, circular faces of the sample and the uniaxial (compressive) loading direction, respectively. We note that there are two characteristic planes of ellipsoidal shape within the specimen that can be constructed by cutting the specimen along a plane through points A and C in the case of the "long diagonal plane", and through points B and D for the "short diagonal plane" (figures 1b and c).

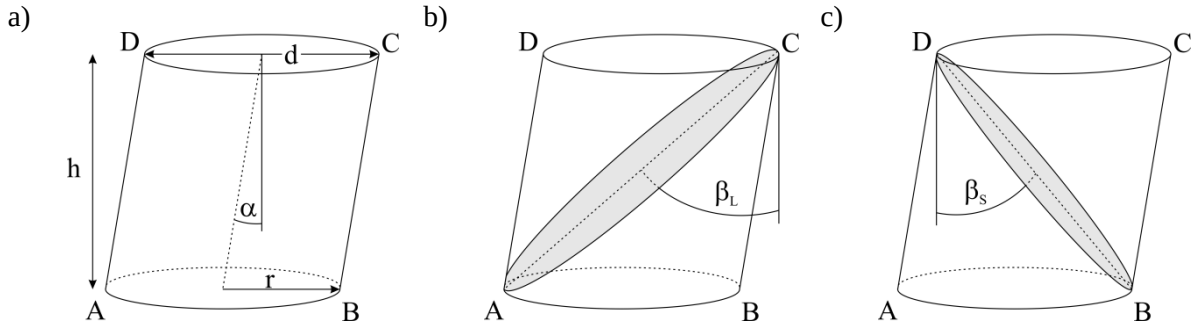

Figure 1. Geometry of the compression-shear specimen (a). Long (b) and short (c) diagonal planes of the specimen can be described by their angles to the vertical axis, β_L and β_S, respectively.

These characteristic planes can also be defined by their angles to the vertical axis, β_L and β_S, respectively. As discussed below, these angles are a function of α. In this study, FE simulations were used to analyze the characteristic stress states in compression-shear experiments for three different (elastic, ideal-plastic) materials, roughly corresponding to three conventional steels: a mild steel S235 with a yield strength of 235 MPa and two tempering steels C45 and 42CrMo4 with yield strengths of 490 MPa and 900 MPa. The elastic constants were assumed to be constant for all three materials, with a Young's modulus of 205 GPa and a Poisson's ratio of 0.3.

3. Analytical assessment of shear stresses

The inclination of the compression-shear specimen leads to a compressive stress state superimposed with a shear stress state when the sample is loaded by a compressive force on its two circular faces. A first approximation of the ratio of shear stresses (in the short diagonal plane) to compressive stresses was derived by Meyer et al. [9, 6], which is simply a function of α and therefore naturally only holds for the undeformed specimen (i.e., during early loading):

$$\tau/\sigma = \tan(\alpha) \tag{1}$$

Equation (1) is, moreover, only valid for frictionless conditions, and it is based on the assumption of constant shear and normal stresses within any plane parallel to the faces of the compression-shear specimen. With similar assumptions, the shear and normal stresses in an arbitrary plane within the specimen (inclined by an angle φ to the vertical axis) can be determined using Mohr's circle [10]. This calculation corresponds to a simple coordinate transformation of the 2D stress state:

$$\sigma_\varphi = -{}^1\!/_2\left(\sigma_{xx}+\sigma_{yy}\right) - {}^1\!/_2\left(\sigma_{yy}-\sigma_{xx}\right)\cos(2\varphi) + \sigma_{xy}\sin(2\varphi) \tag{2}$$

$$\tau_\varphi = {}^1\!/_2\left(\sigma_{yy}-\sigma_{xx}\right)\sin(2\varphi) + \sigma_{xy}\cos(2\varphi) \tag{3}$$

Using the tilt angles of the short and long diagonal planes of the compression-shear specimen, the amount of superimposed shear stress can be estimated for different specimen geometries. Figure 2 shows the tilt angles of short and long diagonal plane for three different specimen aspect ratios and for the experimentally relevant range of inclination angles and d/h ratios. Empty circles represent specimen geometries that were also analyzed using the finite element method in this study (see below). In case of a conventional compression specimen ($\alpha = 0°$) with an aspect ratio of 1 (blue curves), both tilt angles are 45°. Thus, maximum shear stresses occur in these planes during loading. Inclining the specimen leads to an increase of the tilt angle of the long diagonal plane while the tilt angle of the short diagonal plane is decreased. Shear stresses decrease within both planes with increasing angle of inclination due to their increasing deviation from the 45° inclination. An increase of the specimen aspect ratio to 1.25 (orange curves) and 1.5 (pink curves) results in a decrease of both tilt angles. Shear stresses are expected to decrease with increasing specimen aspect ratio for a given angle of inclination. Note that for aspect ratios larger than 1 (and for $\alpha > 0°$), shear stresses in the long diagonal plane are higher than those in the short diagonal plane, because the corresponding tilt angles are closer to 45°. Only small angles of inclination and negligible amounts of friction allow for such a direct estimation of shear stresses with the tilt angle approach according to Mohr's circle. As is discussed in the remainder of this paper, a more accurate analysis of the stress state, also accounting for the effect of different material parameters and friction conditions, can be performed by means of FE simulations.

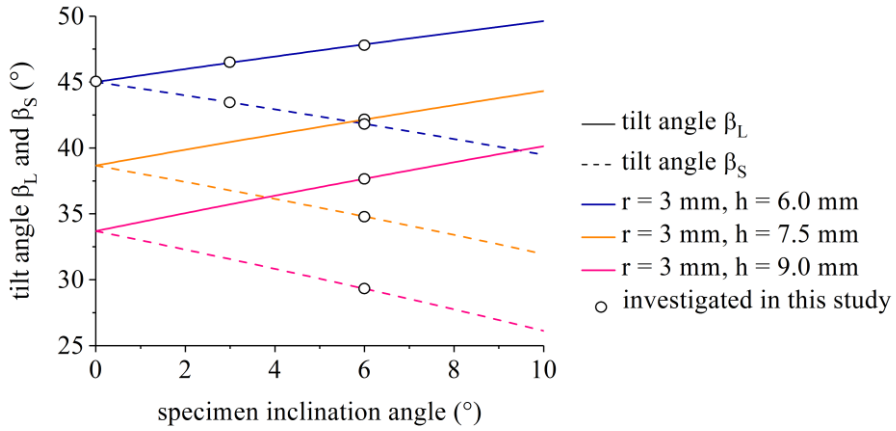

Figure 2. Tilt angles of the short (dashed lines) and long (solid lines) diagonal planes as a function of the inclination angle for compression-shear specimens with different height/diameter ratios. Empty circles mark orientations of the characteristic short and long diagonal planes of specimens that were further investigated in this study.

4. Finite element analysis

In our FE simulations, we systematically considered different specimen geometries with different inclination angles, specimen aspect ratios (height/diameter), friction conditions between tool plates and specimens, and material parameters (yield stresses). All simulations consider an elastic-ideal plastic material behavior with a Young's modulus of 205 GPa and a Poisson's ratio of 0.3. Table 1 provides a summary of the parameter variations used in the different simulations.

Table 1. Overview of the parameters used in the different FE simulations.

μ (–)	d (mm)	h (mm)	α (°)	σ_Y (MPa)	investigated parameter
0	6	6	**0**	490	
0	6	6	**3**	490	angle of inclination
0	6	6	**6**	490	
0	6	**6**	6	490	
0	6	**7.5**	6	490	specimen aspect ratio
0	6	**9**	6	490	
0.05	6	6	6	490	
0.10	6	6	6	490	friction
0.15	6	6	6	490	
0	6	6	6	**225**	
0	6	6	6	**490**	yield strength
0	6	6	6	**900**	

To investigate the multiaxial stress state in a compression-shear specimen subjected to uniaxial load in detail, 3D FE simulations were performed with the FE software package Abaqus, using 26.000 brick elements (C3D8R type) in a static analysis. The tool plates were considered as two rigid surfaces, using node to surface contact with a hard contact in normal direction and a constant friction coefficient in tangential direction. All simulations were stopped when the von Mises stress at any integration point met the static yield strength of the investigated material; our simulation results therefore represent the stress at the onset of yielding in a compression-shear test.

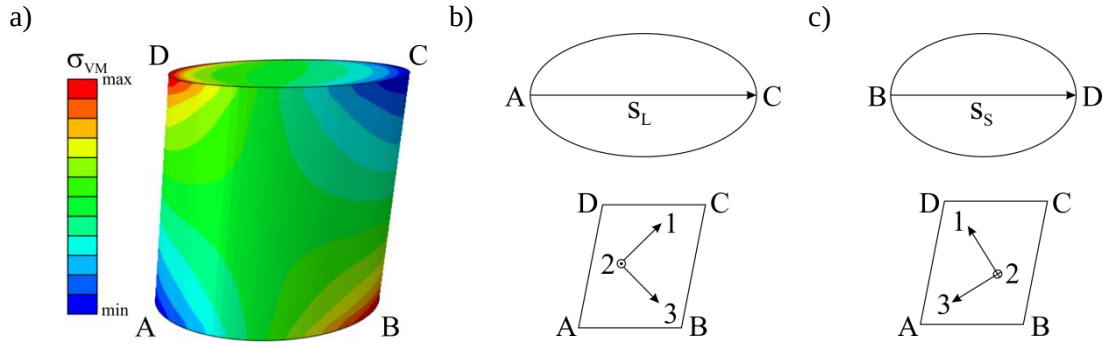

Figure 3. Equivalent von Mises stress distribution on the surface of the inclined compression-shear specimen (a). Long diagonal plane with path s_L and corresponding local coordinate system for shear stress evaluation (b). Short diagonal plane of the compression-shear specimen, path s_S and corresponding local coordinate system (c).

Figure 3a qualitatively shows a representative result valid for all inclined compression-shear specimens (for general validity, the color scale does not indicate distinct stress values since these are a function of the material parameters used in each simulation). The maximum von Mises stress occurs in the edges of the short diagonal plane, whereas minimum von Mises stress values are observed in the edges of the long diagonal plane. Obviously, both planes are interesting for further analysis of the stress state since they represent the limiting cases for the stress states throughout the entire specimen. Figures 3b and 3c schematically show top-down views on the long and short diagonal planes of elliptic shape, with characteristic paths along the long axes of the ellipses s_L and s_S, respectively. Note that s_L (path from point A to C) is longer compared to s_S (point B to D) because of the specimen inclination. The corresponding local coordinate systems are oriented (lower parts of figures 3b and 3c) with respect to the respective paths: 1-directions are parallel to the direction of the investigated path, 3-directions are perpendicular to the path and the 2-directions are oriented following the conventions for right-hand Cartesian coordinate systems.

5. Results and Discussion

In our FE simulations shear stresses τ_{31} were calculated along the two paths (s_L and s_S) of each long and short diagonal plane. Different simulations were performed to investigate the effect of four parameters (see table 1): specimen inclination angle, aspect ratio, friction coefficient between specimen and the tool plates and yield strength of the material. In the following discussion, path lengths are normalized and shear stresses are always related to the corresponding local coordinate system (as defined in figure 3).

5.1 Inclination angle and specimen aspect ratio

Loading of the compression-shear specimen leads to a combined stress state of compression and shear. The inclination angle as well as the specimen aspect ratio control the geometry and therefore also affect the imposed stress state. Figure 4 shows how the shear stresses τ_{31} is varied along the paths in the long and short diagonal planes for different angles of inclination.

It is well-known that in a conventional compression specimen (dotted line) the highest shear stresses occur in planes that are inclined by 45° relative to the longitudinal axis. In this case, the shear stresses are equal to half of the applied normal stress. In the simulations considered here, the normal stress was limited by the yield strength of the material (490 MPa). As a consequence, the shear stress is constant with τ_{31} = 245 MPa along both paths. A specimen inclination of 3° (dashed lines in figure 4) results in a decrease of shear stress along the long diagonal path (figure 4a). Along path s_L shear stresses are low (148.3 MPa) at the edges and increase towards their maximum (198.1 MPa) at the center of the specimen. A similar distribution of shear stresses is observed for 6° of inclination (solid

line), with a maximum of 163.3 MPa in the center and a minimum of 87.7 MPa at the edges. A different shear stress distribution is observed in the short diagonal plane (figure 4b) along path s_S: At the edges, high shear stresses of 250.1 MPa (3° inclination) and 251.7 MPa (6° inclination) arise due to the geometry of the specimen – these stresses are even somewhat higher than the constant shear stress in a conventional compression specimen. These results show that Mohr's circle approach cannot be used to estimate shear stresses, particularly at the edges, of compression-shear specimens. Towards the center of the specimen the shear stresses decrease to minima of 198.0 MPa (3° inclination) and 162.9 MPa (6° inclination), respectively. There is a much higher gradient of the shear stress for the 6° inclination, although both compression-shear specimens exhibit nearly similar shear stresses at the edges of the short diagonal path. We highlight that particularly in less ductile or brittle materials, the formation of cracks, and thus the onset of shear failure, typically occurs at the edges of the short diagonal plane – our results demonstrate that this is a natural consequence of the geometry-imposed increase of stresses in these regions. The shear stresses distributions along both paths are symmetric, with a local maximum/ minimum at the center of the specimen. These shear stress distributions are characteristic for the compression-shear specimen. Clearly, calculating a simple ratio of shear to compressive stresses using the analytical model (see equation 1) cannot accurately represent such stress distributions even though our FE simulations are still limited to the stress states at the onset of plastic deformation only.

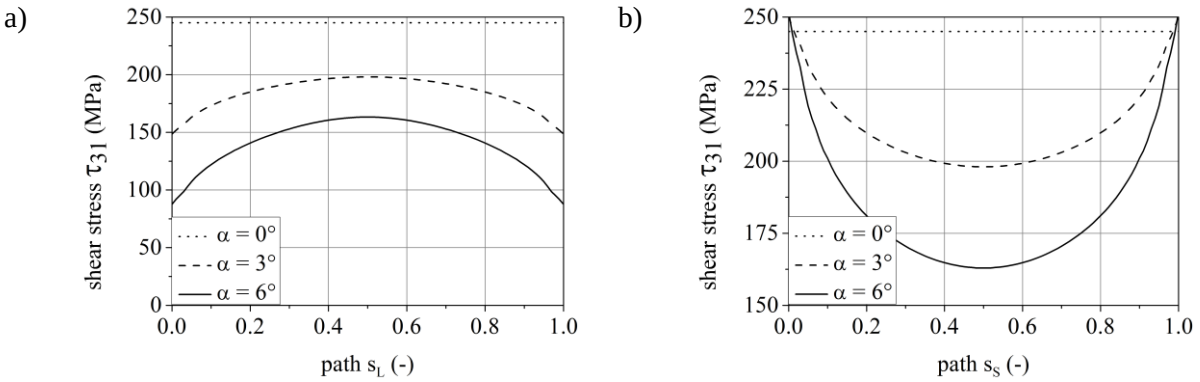

Figure 4. Shear stresses τ_{31} along paths s_L and s_S for a non-inclined compression specimen with inclination 0° (dotted lines) and for two compression-shear specimens with inclinations of 3° (dashed lines) and 6° (solid lines). Aspect ratio h/d: 1, no friction.

An increase of the inclination angle results in an overall decrease of shear stresses along s_L, again with highest shear stresses at the center of the specimen. In contrast, the highest shear stresses arise at the edges of the short diagonal path s_S and decrease towards the center. Moreover, an increasing inclination angle results in an increase of the shear stress gradient. Both paths intersect at the center of the compression-shear specimen, but the shear stresses at this point are not equal. Shear stresses referring to the local coordinate system of the long diagonal plane are slightly higher (198.1 MPa and 163.3 MPa) compared to the shear stresses referring to the local coordinate system of the short diagonal plane (198.0 MPa and 162.9 MPa). This is, of course, in line with Mohr's circle: the tilt angles β_L (46.5° and 47.9°) are closer to 45° (highest shear stresses expected for small inclinations and negligible friction) compared to β_S (43.4° and 41.8°, see figure 2).

Besides the inclination angle, the specimen aspect ratio controls the orientation of long and short diagonal planes and therefore affects the distribution of shear stresses. Figure 5 shows the shear stresses τ_{31} along both long and short diagonal paths for specimen aspect ratios (h/d) of 1 (solid line), 1.25 (dashed line) and 1.5 (dotted line). A similar progress of shear stress curves is visible compared to the inclination angle parameter study along both paths. With increasing specimen aspect ratio, shear stress curves are shifted towards smaller values. This can be documented regarding the maxima and

minima at the center of the specimen (intersection of paths s_L and s_S). For the long diagonal path (figure 5a) maxima are shifted from 163.3 MPa (h/d = 1) to 151.9 MPa (h/d = 1.25) and 139.5 MPa (h/d = 1.5); similarly, minima of τ_{31} on the short diagonal path (figure 5b) change from 162.9 MPa to 137.7 MPa to 115.0 MPa with increasing h/d. Again shear stresses at the center are higher for the long diagonal path, and this observation is in line with Mohr's circle and the corresponding tilt angles (figure 2).

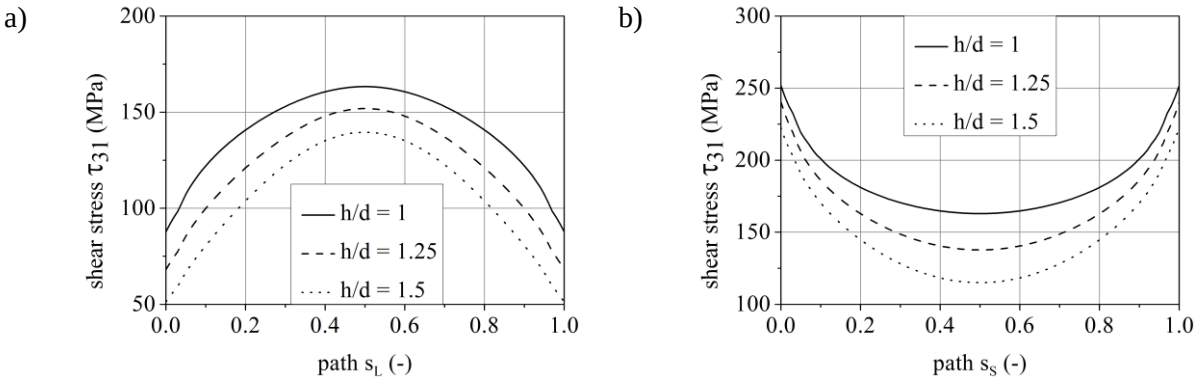

Figure 5. Shear stresses τ_{31} corresponding to the local coordinate systems within long and short diagonal planes for different specimen aspect ratios (h/d), a constant inclination angle of 6° and no friction. Solid lines refer to the specimen aspect ratio of 1, dashed and dotted lines to 1.25 and 1.5, respectively.

5.2 Friction

Friction between the tool plates and the specimen surfaces was neglected in all numerical investigations discussed above. In the FE analysis considered next, the tool plates have been defined as rigid surfaces with hard contact in normal and a constant Coulomb friction coefficient μ in tangential direction. Figure 6 shows the shear stresses τ_{31} along the two paths s_L and s_S within the long and short diagonal planes for different coefficients and a constant inclination angle of 6° as well as a specimen aspect ratio of 1. Again, shear stresses correspond to the local coordinate system of each plane (figure 3).

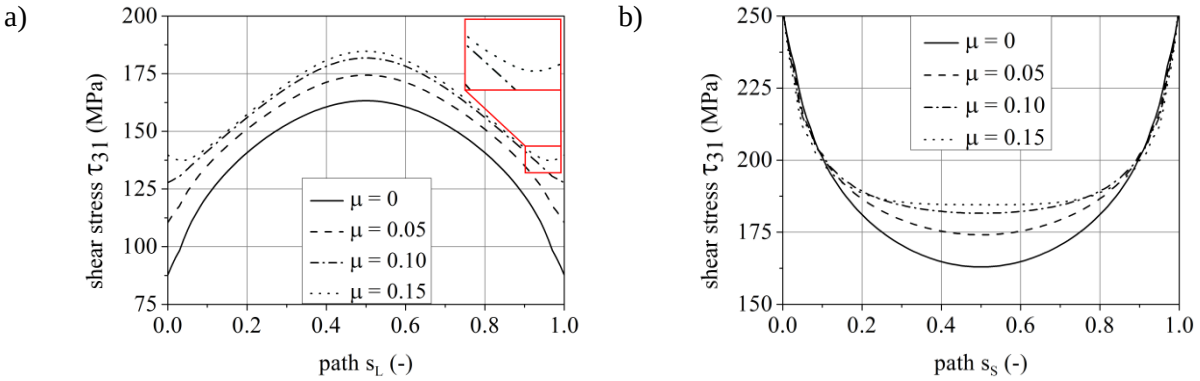

Figure 6. Shear stresses τ_{31} according to the local coordinate system of long and short diagonal plane along the corresponding paths. Results with different friction coefficients in tangential direction $\mu = 0$ (solid line), $\mu = 0.05$ (dashed line), $\mu = 0.10$ (dash-dotted line) and $\mu = 0.15$ (dotted line) are shown.

A similar trend of the curves compared to the results discussed in subsection 5.1 is observed. An increase of the friction coefficient ($\mu = 0$, solid line; $\mu = 0.05$, dashed line; $\mu = 0.10$, dash-dotted line

and $\mu = 0.15$, dotted line) results in an increase of the absolute shear stress values because a higher normal stress is required to overcome tangential friction. Within the long diagonal path (figure 6a) shear stresses increase at the edges from 87.7 MPa ($\mu = 0$) to 139.7 MPa ($\mu = 0.15$). Note that there is a local minimum for the highest friction coefficient $\mu = 0.15$ (inset in figure 6a). At the center of the specimen, the shear stresses also increase from 163.3 MPa ($\mu = 0$) to 184.8 MPa ($\mu = 0.15$). Since the maximum values in the center for high friction coefficients are nearly similar, it is not expected that a further increase of the friction coefficient considerably changes the shear stresses near the center of the specimen. For the short diagonal path (figure 6b) the shear stresses are very similar at the edges of the path s_S. In the center region of the path (0.2 – 0.8), however, the curves differ: an increase of the friction coefficient results in an increase of shear stress values and the shear stress gradient decreases. Shear stresses change from 162.9 MPa ($\mu = 0$) to 184.6 MPa ($\mu = 0.15$) in the center. It is again expected that a further increase does not change the shear stress in the center of the specimen. These findings demonstrate that the friction coefficient has a strong impact on the shear stress gradient along both paths. Moreover, shear stresses are generally increased compared to a simple scenario where friction is neglected.

5.3 Yield strength

Figure 7 shows the shear stresses along both path s_L and s_S for different (constant) yield strengths σ_Y. A mild steel with $\sigma_Y = 235$ MPa (solid line) and two tempering steels C45 with $\sigma_Y = 490$ MPa (dashed line) and a 42CrMo4 with $\sigma_Y = 900$ MPa (dotted line) were considered as model materials.

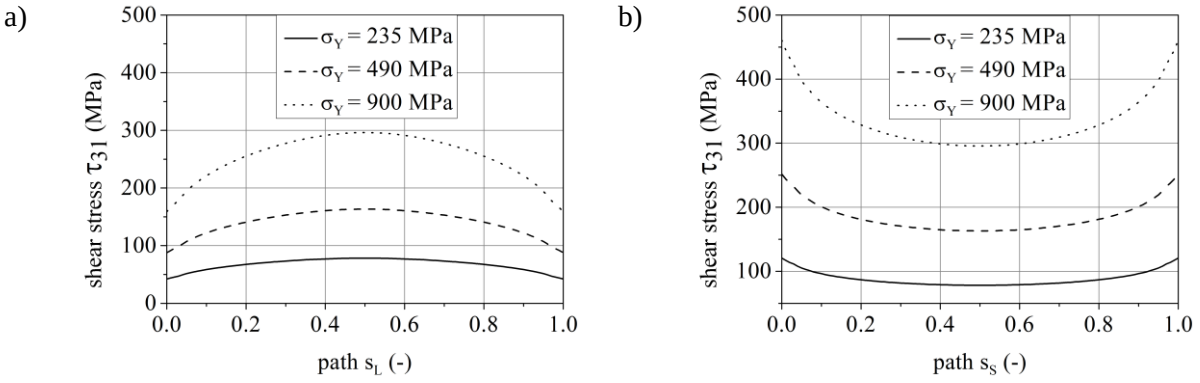

Figure 7. Shear stresses τ_{31} along the paths within the long and short diagonal plane for different yield strength values; solid line ($\sigma_Y = 235$ MPa), dashed line ($\sigma_Y = 490$ MPa), dotted line ($\sigma_Y = 900$ MPa).

Shear stresses along the long diagonal path (figure 7a) are still lower at the edges with a maximum in the center of the specimen. In contrast, shear stresses along the short diagonal path (figure 7b) are lowest at the center of the specimen and increase towards the edges of the path. An increase of the yield strength results in an increase of shear stresses. This is of course due to the need for higher normal stresses as our simulations were stopped when the yield strength was reached at any integration node in the specimen. We also find that an increase of yield strength results in an increase of the shear stress gradients along both paths.

6. Summary and conclusions

Based on simple 3D elastic-ideal plastic FE simulations, we performed an analysis of the stress state at the beginning of plastic deformation in the compression-shear specimen introduced by Meyer [5]. We systematically investigated the impact of specimen inclination angles, specimen aspect ratios, and friction coefficients between the tool plates and the specimen surfaces, as well as the effect of different yield strengths of the material. Since they play a key role in deforming the material in a compression-shear test, shear stress distributions were analyzed in detail taking local coordinate systems oriented parallel to short vs. long diagonal planes into account. The results provide detailed information on the stress state during early loading; they can be summarized as follows:

- During uniaxial, compressive loading of the compression-shear specimen, a geometry imposed combined stress state of superimposed compression and shear loading occurs. The highest equivalent von Mises stresses are observed at the edges of the short diagonal plane, whereas the lowest von Mises stresses occur at the edges of the long diagonal plane.
- In the center of the specimen, where both planes intersect, different shear stresses are determined in each plane. Shear stresses in the long diagonal plane are always higher compared to those in the short diagonal plane. This can be explained by the different tilt angles of these planes with respect to the loading axis.
- An increase of the inclination angle, and/ or an increase of the specimen aspect ratio results in an increase of shear stresses in both planes. Moreover, the shear stress gradients increase with increasing inclination angle.
- Larger amounts of friction result in higher shear stresses and lower gradients in the center region of the short diagonal path and also in the long diagonal path. Moreover, the yield strength of the material has no significant influence on the resulting shear stress distributions, but an increase of the yield strength leads to an increase of shear stress gradients along both paths.

References

[1] Rittel D, Lee S and Ravichandran G 2002 *Exp. Mech.* **42** 58
[2] Sang D-L, Fu R-D and Li Y-J 2016 *Mater. Charact.* **122** 154
[3] Moemeni S, Zarei-Hanzaki A, Abedi H R and Torabinejad V 2012 *Exp. Mech.* **52** 629
[4] Ashab A S M , Ruan D, Lu G and Wong Y C 2016 *Mater. Design* **97** 183
[5] Meyer L W, Staskewitsch E and Burblies A 1994 *Mech. Mater.* **17** 203
[6] Meyer L W and Pursche F 2011 *Engineering Transactions* **59** 21
[7] Elibol C and Wagner M F-X 2015 *Mat. Sci. Eng.* A **621** 76
[8] Elibol C and Wagner M F-X 2015 *Mat. Sci. Eng.* A **643** 194
[9] Meyer L W and Krüger L 2007 *ASM Handbook* vol 8 (Ohio: ASM International) pp 452–4
[10] Salençon J 2001 *Handbook of continuum mechanics* (Berlin: Springer) p 266